https://ntrs.nasa.gov/search.jsp?R=19850005823 2020-03-20T19:43:06+00:00Z

PRELIMINARY INVESTIGATION OF LABYRINTH PACKING PRESSURE DROPS AT ONSET OF SWIRL-INDUCED ROTOR INSTABILITY

E. H. Miller and J. H. Vohr
General Electric Company
Schenectady, New York 12345

Backward and forward subsynchronous instability has been observed in a flexible model test rotor under the influence of swirl flow in a straight-through labyrinth packing. The packing pressure drop at the onset of instability was then measured for a range of operating speeds, clearances and inlet swirl conditions.

The trend in these measurements for forward swirl and forward instability is generally consistent with the short packing rotor force formulations of Benchert and Wachter[1].

Diverging clearances were also destabilizing and had a forward orbit with forward swirl and a backward orbit with reverse swirl.

A larger, stiff rotor model system is now being assembled which will permit testing steam turbine-type straight-through and hi-lo labyrinth packings. With calibrated and adjustable bearings in this new apparatus, we expect to be able to directly measure the net destabilizing force generated by the packings.

INTRODUCTION

Destabilizing packing force measurement obtained by integrating circumferential and axial pressure distributions have been reported by several investigators[1,2,3,4] and serve to calibrate various analytical packing force prediction methods[5,6,7,8]. One investigator[9] Wright has reported success in making direct force measurements on a rotor system and in separating the destabilizing cross coupled direct force from the viscous damping forces.

To demonstrate the importance of inlet swirl in the generation of destabilizing packing forces, a rotor packing model with very simple instrumentation was built and tested in our laboratory. With inlet swirl velocities greater than packing surface speed and in the same direction, the rotor became unstable at its first critical speed. Shaft rotation was reversed and the rotor again became unstable with about the same pressure drop across the packing. In this case, however, the subsynchronous orbit continued rotating in the direction of inlet swirl opposing the direction of shaft rotation.

We then modified the packing model and with additional instrumentation, carried out a limited test program to measure the pressure and flow conditions which would cause instability with

alternate packing designs. These tests have the virtue that both direct and damping forces are physically integrated by the rotor. They have the disadvantage that, with the bearings and instrumentation used in this program, we could not quantify the level of the destabilizing force nor could we separate the direct from the damping forces to make comparisons with published data.

Discussion of Initial Test Results

Figure 1 shows the assembled rotor/labyrinth facility. The two flexible air hoses are independently valved to permit either forward or backward swirl without changing shaft rotation. By opening both valves together the inlet velocities are essentially cancelled and a test condition of negligible swirl exists. While the preliminary tests had used a single admission with reversed motor rotation to get backward swirl, the two admission modification greatly simplified the test procedure and analysis.

Figures 2 and 3 show the rotor and labyrinth components of this facility. Air is admitted to the central plenum through the tangential inlets. Pitot tubes installed in the plenum measured the swirl velocity. Two static pressure taps are also located in the inlet plenum.

The first series of tests were to determine if there was a strong rotational speed dependency. As shown by Figure 4, we did not find any. In future test programs we will measure the bearing dynamic characteristics over the speed range so that we can learn if the apparent larger packing forces at low speed is a real effect.

A typical vibration spectrum at the onset of instability is displayed on Figure 5 for a backward swirl. Filtered synchronous and subsynchronous orbits were simultaneously displayed and forward and backward orbits were easily distinguished. Figure 6 shows this display for the typical backward swirl condition.

Figure 7 shows some particularly interesting data. Both forward and reverse admission valves were fully opened to the shop air supply. The plenum chamber built up to 15 psia and the rotor remained "stable" by previous criteria. When the instrument gain was increased by 10X, a non-synchronous orbit was observed at about 15 Hertz, sometimes rotating in the synchronous direction sometimes against.

The initial tests were run at .010 radial clearance on all the teeth. The packing casing was then disassembled without disturbing the rotor and bearings, and the clearances were enlarged in a diverging geometry from .010" at the packing inlet to .020 mils at the exit. The third and last test of the clearance series was with the clearances further enlarged to a cylindrical .020" clearance. The data for the six test conditions are show on Figure 8. Since there has been much conjecture about the "stabilizing" effect of diverging clearance, special attention was given to the diverging test condition. In addition to the usual visual examination of orbits on the CRT, analysis of the signal confirmed that the

subsynchronous orbit with diverging clearance packings was in the same direction as inlet swirl and, in all respects, the diverging 10/20 mil clearance case behaved like an intermediate clearance between 10 and 20 mils.

The raw data is misleading in indicating a lower critical pressure, hence, a higher level of instability- as clearances are increased. This effect is related to our test model, since as clearances are increased the inlet velocity also increases and this increases inlet swirl. Benchert and Wachter's[1] short packing formula shows packing force increasing proportionally with inlet pressure and inlet swirl energy. Using average tangential velocities from our pitot data and the referenced force formulation, we have corrected the raw trend line of Figure 7 to a constant inlet swirl condition.

A further test was carried out to assess the effect of swirl, independent of clearance. The labyrinth packing casing was modified with temporary nozzle liners in the inlets and tests were repeated at the .010 mil clearance but now with higher nozzle inlet velocities. The results of these tests are shown on Figure 9 and confirm the strong correlation between destabilizing force and inlet swirl velocity.

PROPOSED TEST PROGRAM

As noted earlier, it was not possible to obtain a quantitative determination of destabilizing forces contributed by the packings because the flexible shaft and the unknown and asymmetrical cross coupling stiffness forces of the cylindrical bearings. In a future series of tests, this problem will be remedied by using a stiff test rotor supported on tilting pad bearings with adjustable, isotropic calibrated stiffness and damping characteristics. A picture of the test facility is shown in Figure 10.

This facility was originally designed for dynamic testing of bearings but is being modified by replacing the midspan test bearing with an appropriate labyrinth test seal and by installing the special isotropic support bearings. A schematic of the test rig is shown in Figure 11. Air is introduced into a central plenum, passes through the labyrinth and exhausts to atmosphere at either end. Various seal configurations and clearances will be tested. The air in the plenum will be introduced with controlled and measured swirl.

The tilting pad support bearings are mounted on springs having a stiffness value of approximately 2.3×10^4 lb/in. Two pads at each end of the rotor are oriented at 45° from vertical, resulting in isotropic stiffness and damping characteristics; i.e., vertical and horizontal stiffness are the same. Use of tilting pads eliminates any destabilizing cross coupling stiffness coefficients from the bearings.

For such an isotropic system, the force balance at the threshold of instability is:

$$K_S = (B_b + B_s)\nu$$

where K_S is the destabilizing cross coupling stiffness force generated by the test seal, B_b is the isotropic damping coefficient of the spring mounted support bearings, B_S is the damping coefficient of the seal and ν is the natural frequency of the rotor on its support bearings. Because the tilting pad bearings are mounted on springs whose stiffness is relatively low compared with the stiffness of the oil film between the pad and the rotor, the effective damping B_b of the oil film and support spring in series is quite low and may be varied by changing the vertical load imposed on the shaft as shown in Figure 12. Test procedures would establish a desired level of damping B_b in the test rig by imposing the appropriate load, bring the rotor up to the desired test speed, and then slowly increase the plenum pressure in the test seal up to the onset of whirl. The net destabilizing force from the seal, $(K_S - B_S)\nu$, will then be determined from the equation above. Damping of the support bearings, B_b, can be determined either by measuring the exponential decay of shaft vibration induced by striking the test rotor or by measuring the response of the rotor to a known unbalance.

A recognized deficiency of the proposed testing is that it will not yield separate determination of K_S and B_S, but only a measurement of the net destabilizing effect of the seal. However, the tests will suffice to check the ability of various analyses to predict this overall destabilizing force permitting one to evaluate the usefulness of these analyses as design tools.

ACKNOWLEDGMENT

The authors acknowledge the substantial assistance of L. L. Bethel and S. K. Tung in all phases of this rotor stability investigation.

REFERENCES

1. Benchert, H.; and Wachter, J.: Flow Induced Spring Constants of Labyrinth Seals, I. Mech. E., Sept. 1980.

2. Leong, Y.; and Brown, R.: Circumferential Pressure Distribution in a Model Labyrinth Seal, NASA CP-2250, 1982, pp. 223-241.

3. Childs, D.; and Dressman, J.: Testing of Turbulent Seals for Rotordynamic Coefficients, NASA CP-2250, 1982, pp. 157-171.

4. Greathead, S.; and Slocombe, M.: Further Investigations into Load Dependent Low Frequency Vibration of the High Pressure Rotor on Large Turbo-Generators, I. Mech. E., Sept. 1980.

5. Iwatsubo, T.; et al.: Flow Induced Force of Labyrinth Seal, NASA CP-2250, 1982, pp. 205-222.

6. Murphy, B; and Vance, J.: Labyrinth Seal Effects on Rotor Whirl Instability, Proceedings I. Mech. E., 1980.

7. Kurohashi, M.; et al.: Spring and Damping Coefficients of Labyrinth Seals, Proceedings I. Mech. E., 1980.

8. Kostyuk, A.: Theoretical Analysis of Aerodynamic Forces in Labyrinth Glands of Turbomachines, Teploenergetika, 1972.

9. Wright, D. V.: Air Model Tests of Labyrinth Seal Forces on a Whirling Rotor, Eng. Power, Oct. 1978.

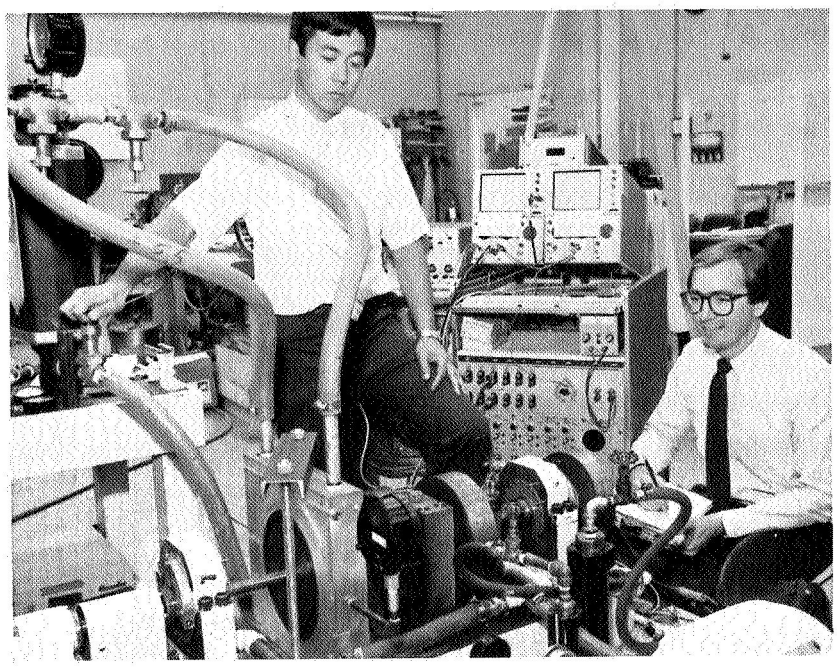

Figure 1. - Assembled rotor and labyrinth packing facility.

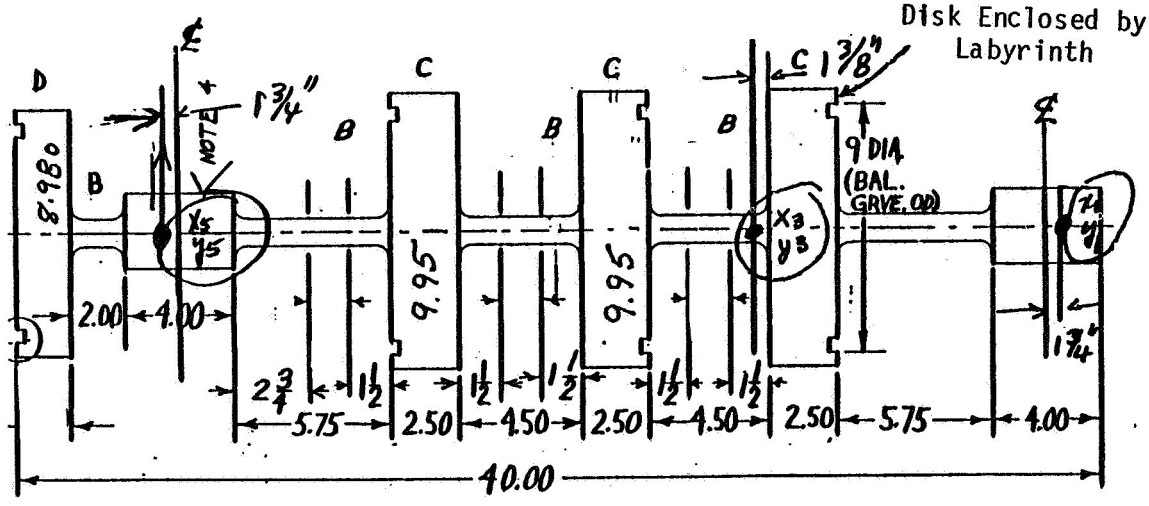

Figure 2. - Schematic of rotor for packing stability test.

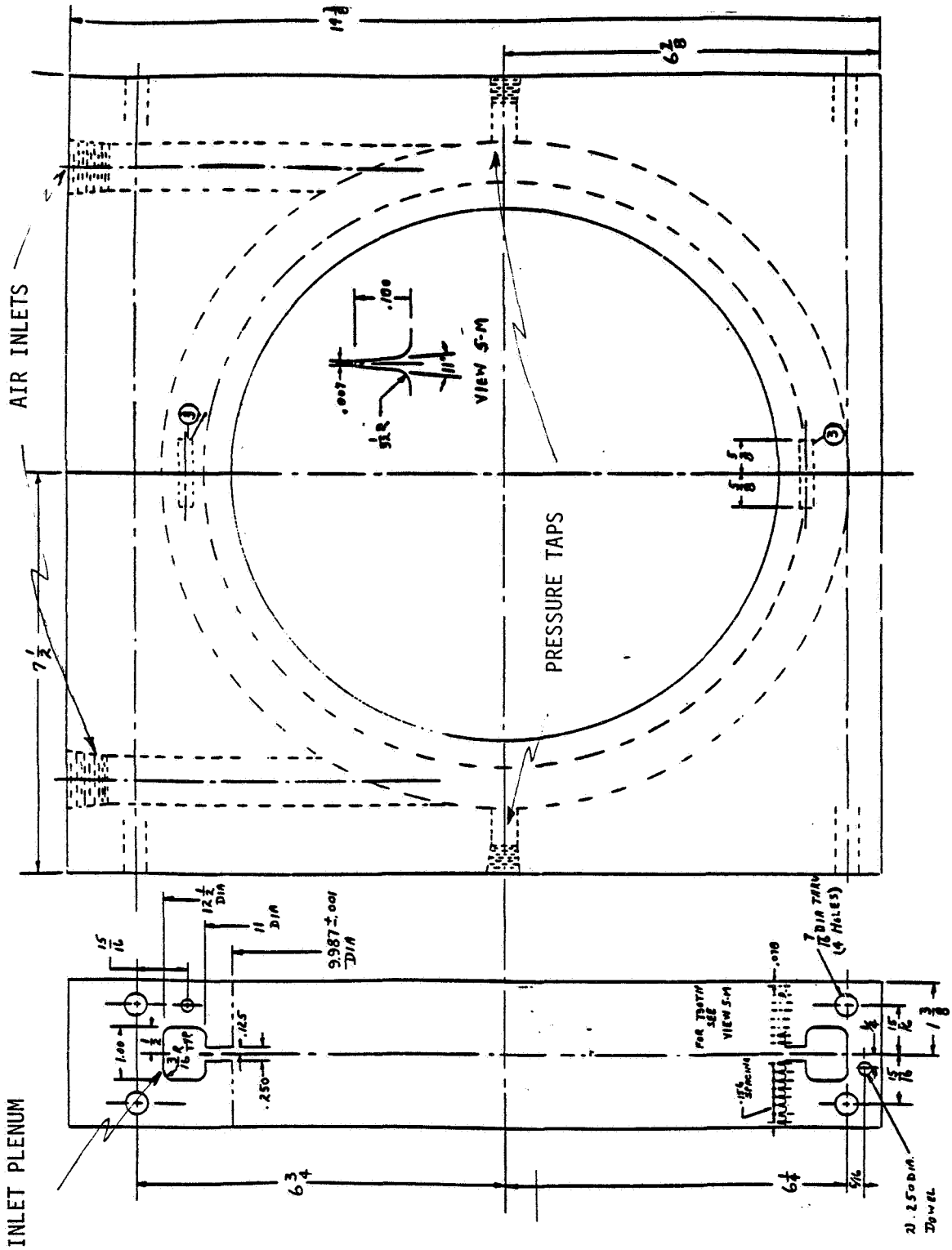

Figure 3. - Schematic of labyrinth for packing stability test.

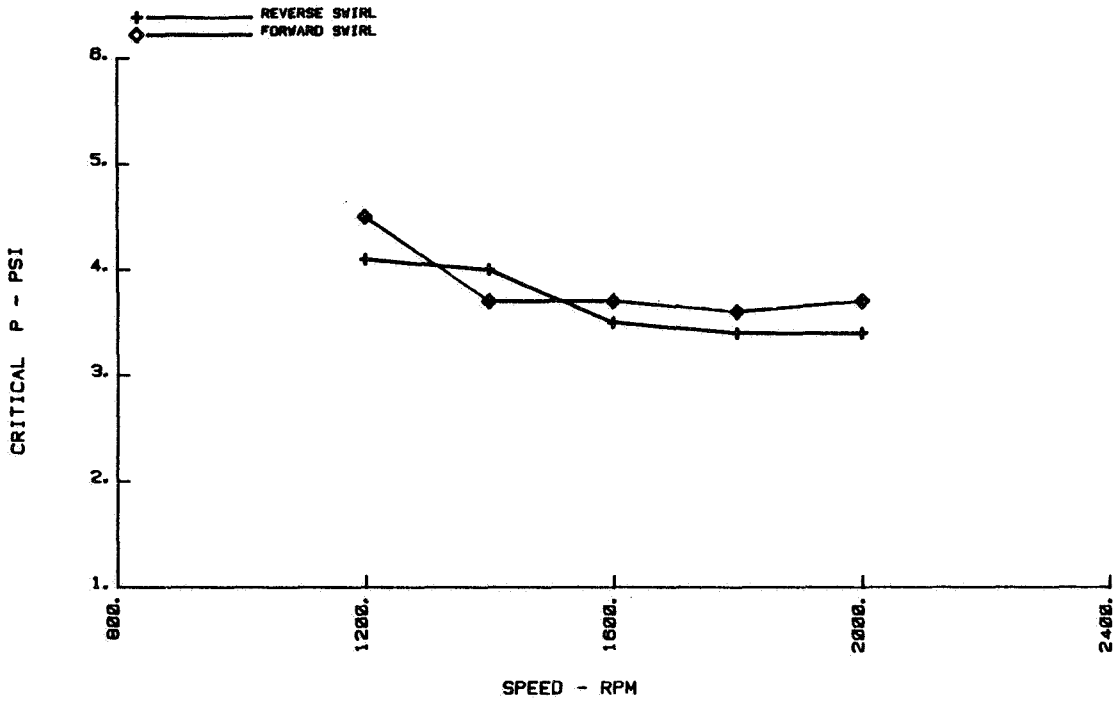

Figure 4. - Threshold pressure drop at various rotational speeds.

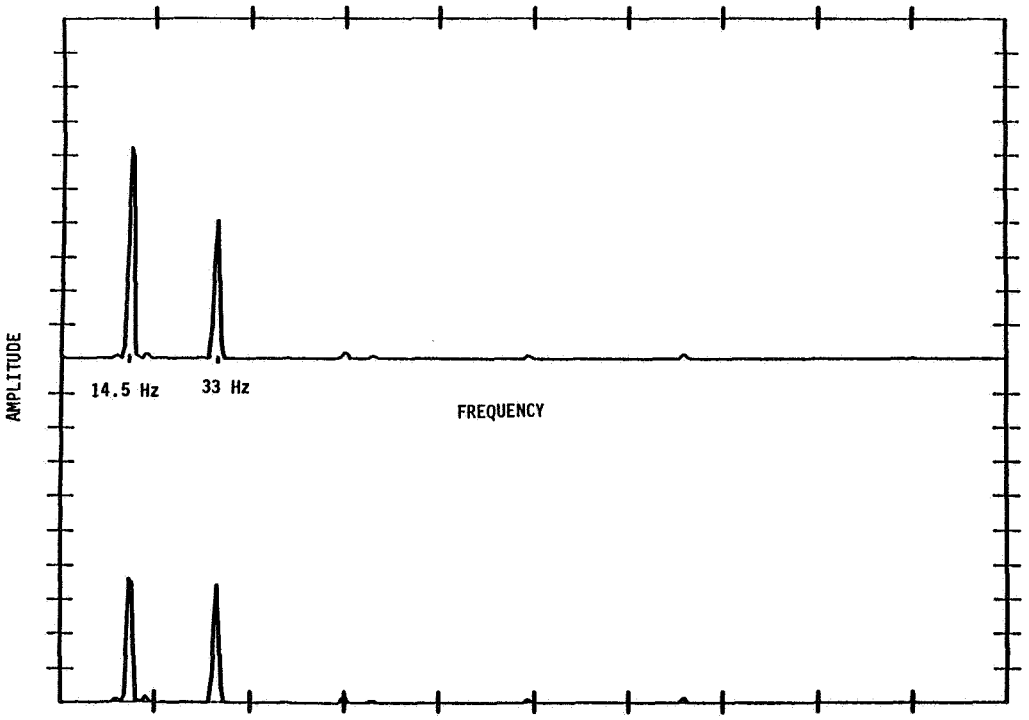

Figure 5. - Typical CCW admission vibration spectrum for packing stability test; CW rotation, 2000 rpm; 4 psi; CCW inlet.

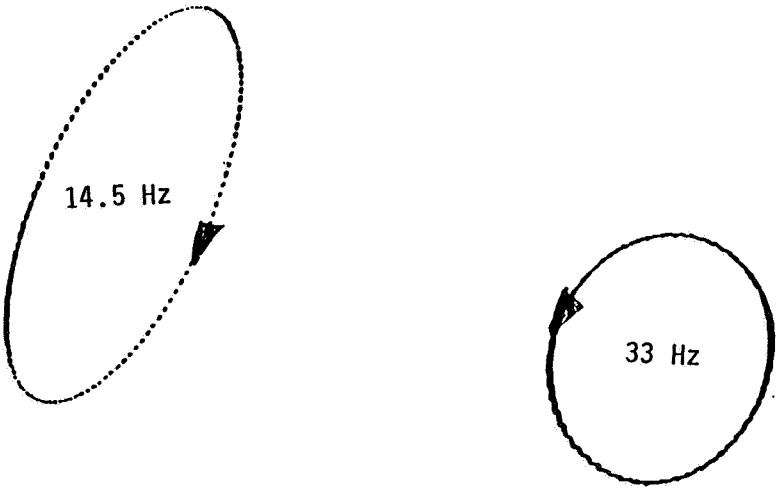

Figure 6. - Typical CCW admission orbits for packing stability test; CW rotation; 2000 rpm; 4 psi; CCW inlet.

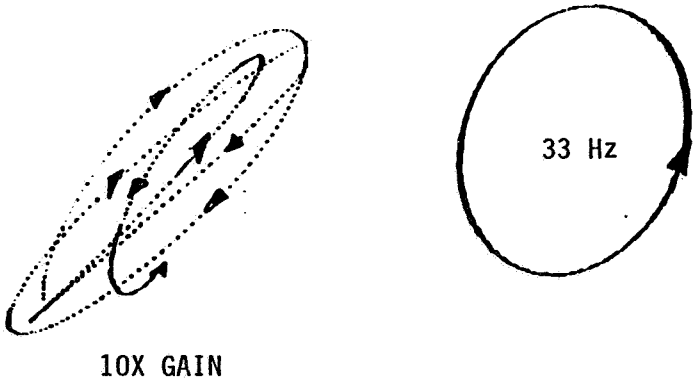

Figure 7. - CW and CCW admission orbits for packing stability test; CW rotation; 2000 rpm; 15 psi; both inlets fully open.

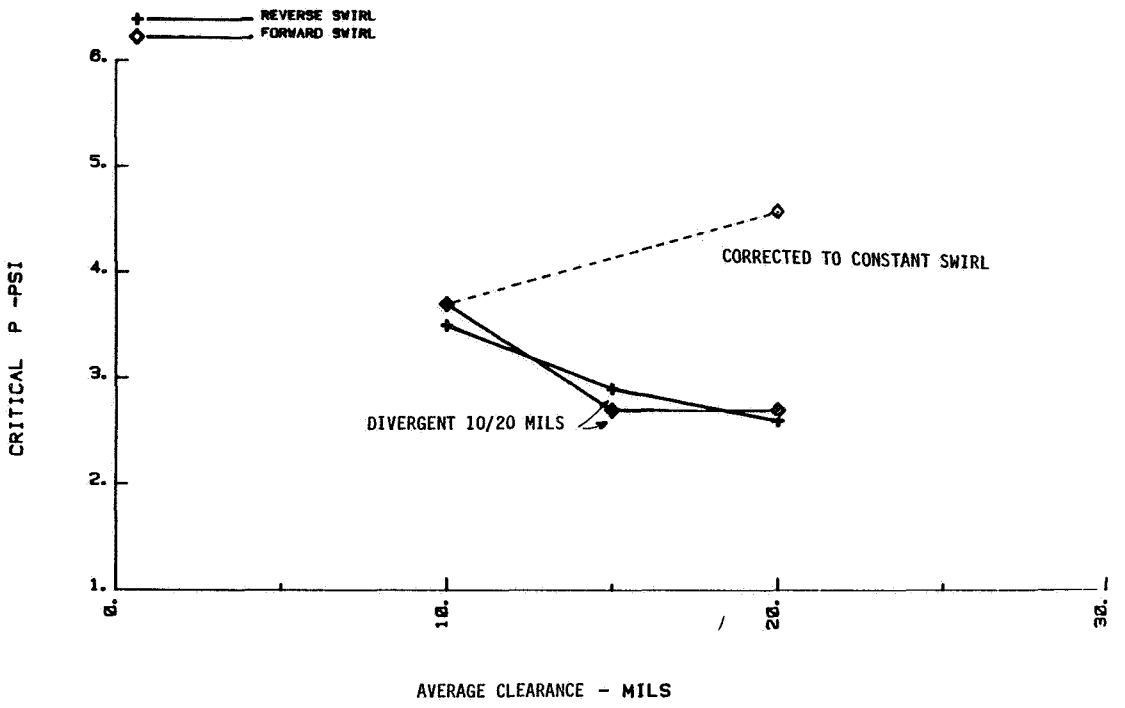

Figure 8. - Threshold pressure drop at various clearances. 1600 rpm.

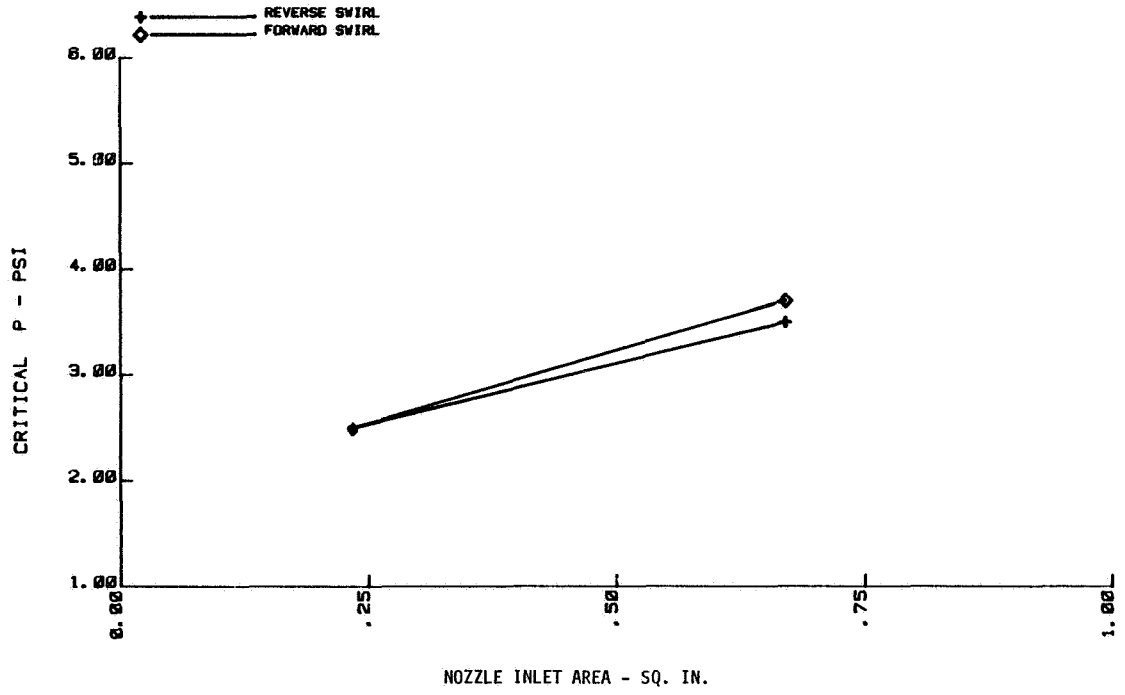

Figure 9. - Threshold pressure drop at alternate inlet areas. 1600 rpm.

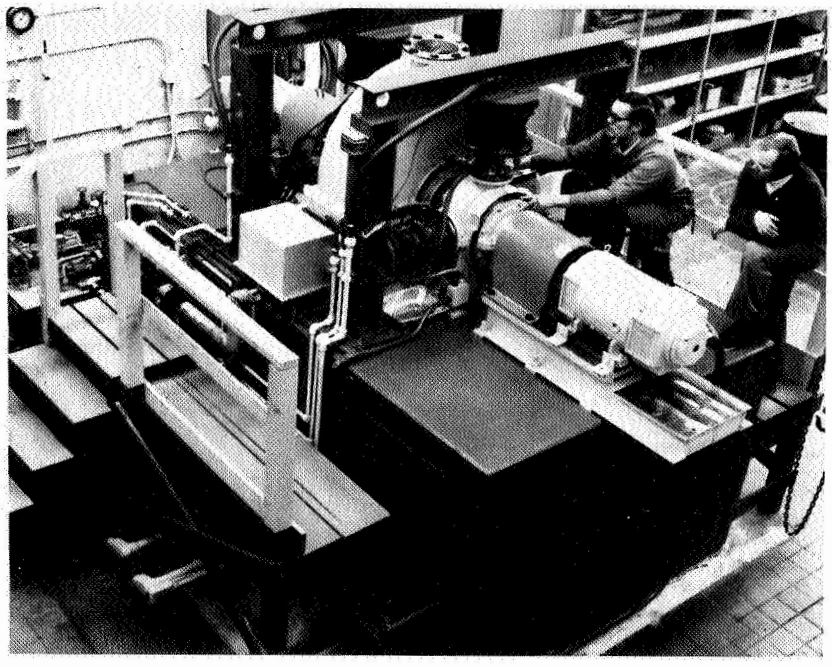

Figure 10. - Large-stiff-rotor labyrinth packing facility.

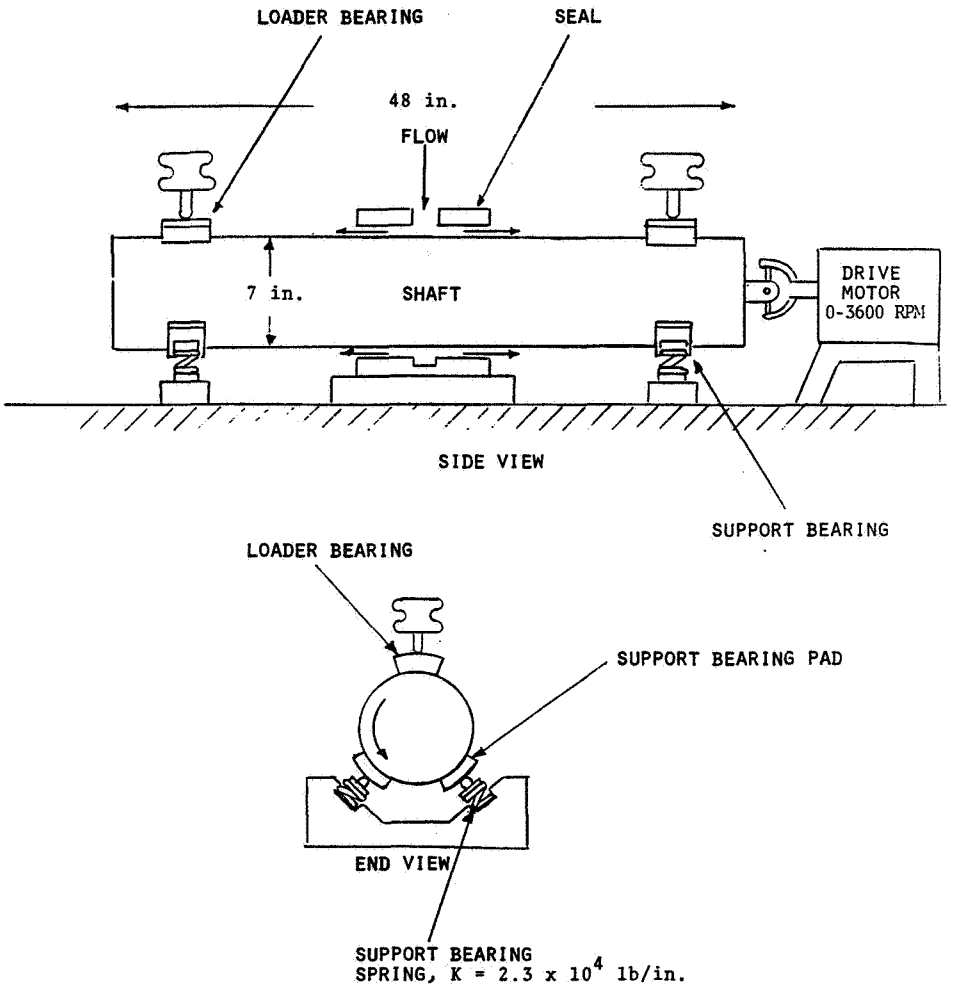

Figure 11. - Schematic of seal force test rig.

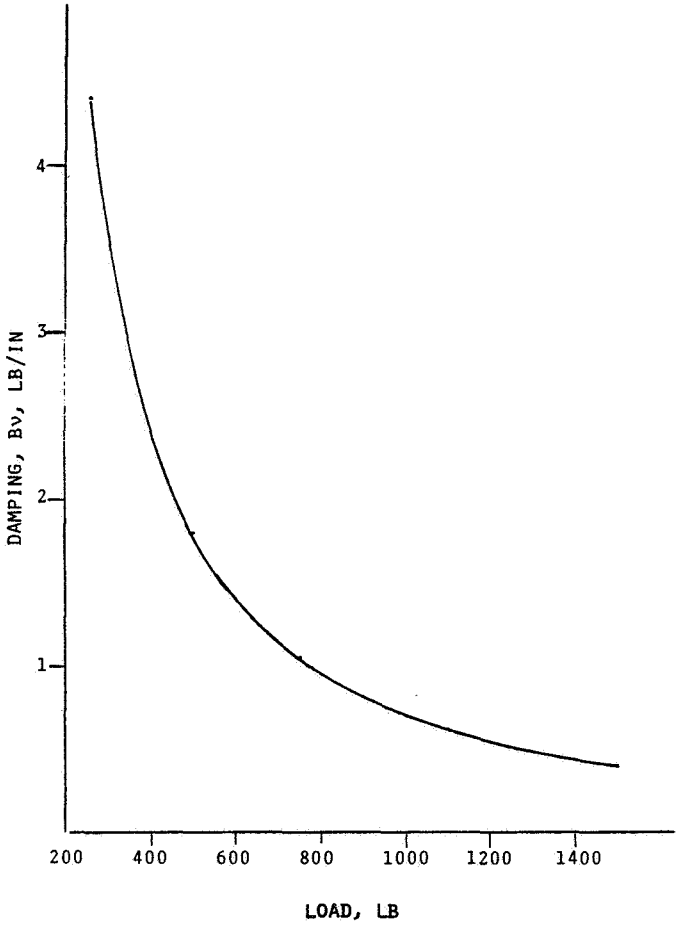

Figure 12. - Test rig damping at various bearing loads.